# Annexes

# A. Electromagnetic design

## A.1 Resistance and inductance of circular coil

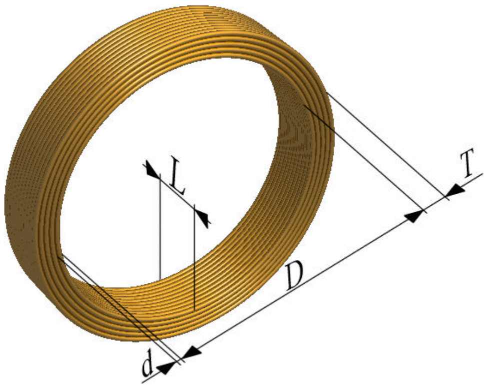


Figure 8: Geometry of a circular coil

| | |
|---|---|
| d | wire diameter |
| ϕ | diameter of wire's conductive area |
| $t_{isolation}$ | thickness of wire's isolation |
| l | total wire length |
| D | core diameter |
| L | coil length |
| T | winding thickness |
| m | # of layers |
| N | # of windings |
| n | # of windings per layer |

Table 1: Symbols

$$f = d - 2t_{isolation} \qquad L = nd \qquad T = md \qquad N = mn$$

### Analytic calculation

The following formulas give a quick overview of coil characteristics. Analytically, the resistance R can be determined accurate but the inductance L only at about ±20%.

Resistance: $R = r\dfrac{4l}{p f^2}$ where $l = Np(D + md)$

$$R = r\frac{4N(D+md)}{f^2} \tag{1}$$

Inductance:

$$L \approx m_0 \frac{pD^2N^2}{2\sqrt{4L^2 + pD^2}} \tag{2}$$

### Numeric calculation

For better accuracy, a numerical analyse software like *MatLab* is useful to give a numerical solution of the inductance L. Below, exact analytic formulas are established and then translated for numerical integration.

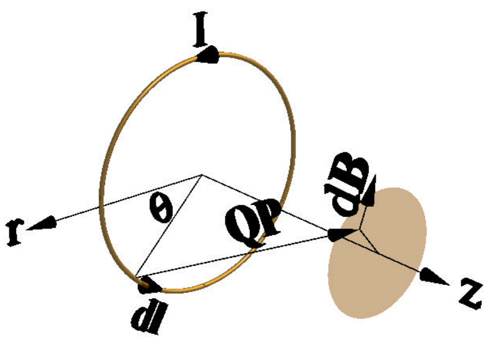


Figure 9: Contribution of current element d**l** at point Q to magnetic field d**B** at point P.

| | |
|---|---|
| I | current in winding |
| B | magnetic flux |
| R | winding radius |
| r | radius |
| θ | azimuth |
| z | axial position |
| d**l** | current element |
| d**B** | magnetic flux incremental |
| **QP** | vector from current element to field point |

Table 2: Symbols [26]

General case: $\overrightarrow{dB} = \dfrac{m_0 I}{4p}\dfrac{\vec{dl} \times \vec{QP}}{\overline{QP}^3}$

[26] Vectors are noted bold or with superior flash.

Inductance: $L = \frac{d\Phi_{tot}}{dI}$ where $\Phi_{tot} = \sum_{i=1}^{N} \iint_S \vec{B_i} \bullet d\vec{s} = m \sum_{k=0}^{n-1} \iint_S \vec{B_k} \bullet d\vec{s}$ (3)

expresses total magnetic flux through the coil.

It will be necessary to determine the flux contribution of each winding through the common circular section S of diameter D of all windings [27].

Note that only the axial field $B_z$ contribute to $\Phi_{tot}$ and that circular symmetry makes sufficient to calculate $B_{k(r)}$ for $r \in [0,D/2]$ and where $z=dk$, $k \in [0,n-1]$. $B_{k(r)}$ denotes the sum of contributions of all m windings in the same section.

Calculate the contribution $B_{k,i(r)}$ of one standalone winding with radius $R=(D+di)/2$. Applying the general case formula results in:

Field point: $\overrightarrow{QP} = \begin{pmatrix} r\cos q - R \\ r\sin q \\ z \end{pmatrix}$

Wire element: $\vec{dl} = \begin{pmatrix} -R\sin q \\ R\cos q \\ 0 \end{pmatrix} dq$

Axial field: $dB_{z(R,r,q,z)} = \frac{m_0 I}{4p} \frac{\left(\vec{dl} \times \overrightarrow{QP}\right)_z}{\overline{QP}^3} = \frac{m_0 I}{4p} \frac{(R - R\cos q)Rdq}{\left(R^2 + r^2 + z^2 - 2rR\cos q\right)^{1.5}}$

$$B_{k,i(r)} = \int_{-p}^{+p} dB_{z(R=(D+id)/2, r, q, z=kd)}$$

Express the magnetic field from m windings in the same section:

$$B_{\mathrm{k(r)}} = \sum_{\mathrm{i}=1}^{m} B_{\mathrm{k,i(r)}}$$

Integrate it over the common section S to get the partial axial flux:

$$\Phi_k = \int_0^{D/2} 2prB_{\mathrm{k(r)}}dr$$

Finish by summing up contributions of each section to each other:

$$\Phi_{tot} = m \sum_{i=0}^{n-1} \sum_{k=-i}^{n-1-i} \Phi_{|k|} = m\left(n\Phi_0 + 2\sum_{k=1}^{n-1}(n-k)\Phi_k\right) \quad (4)$$

It follows the listing of a *MatLab* function which approaches integrals by the piecewise trapezoidal integration formula:

```
% Determines inductance of a circular coil with
% core diameter D, wire diameter d, m layers with
% n windings each.
%
function L=circularInductance(D, d, n, m)
if d < 0 | D < 2*d | n < 1 | m < 1
   L=0;
else
   n=fix(n);
   m=fix(m);
   if n == 1
      L=m*zFlux((D+d)/2, D/2, 0);
   else
      L=zFlux((D+d*(1:m))/2, D/2, d*(0:n-1));
      if m > 1, L=sum(L); end;
      L=m*L*[n 2*(n-1:-1:1)]';
   end;
```

27 Assume no (axial) magnetic field at the interior of wires and between them.

```
end;

% Determines total magnetic flux through a circular
% section A=pi*r*r in an axial distance z from the
% circular winding of radius R where current flows.
%
% Result matrix F gives in its columns total flux
% for different R and in its rows for different z.
%
function F=zFlux(R, r, z)
h=r/25;
r=h*(0:24);
c=2*pi*h*(r+h);
for i=1:length(R)
   F(i,:)=c*zField(R(i), r, z)';
end;

% Determines magnetic flux density at radius r and
% axial distance z from circular winding of radius R
% where current flows.
%
% Result matrix B gives in its columns flux density
% for different r and in its rows for different z.
%
function B=zField(R, r, z)
h=pi/25;
t=h*(-25:24)';
a=cos(t)*r;
b=repmat(r.^2, size(t))+R^2-2*R*a;
c=h*R/10^7;
a=R-a;
for i=1:length(z)
   B(i,:)=c*sum(a./(b+z(i)^2).^1.5);
end;
```

### Comparison

| Coil layout | Analytic: L [H] | Numeric: L [H] | Relative error [%] |
|---|---|---|---|
| D=10cm, d=1mm, n=m=1 | 111n | 256n | –57 |
| D=10cm, d=1mm, n=20, m=1 | 43.5μ | 62.9μ | –31 |
| D=10cm, d=1mm, n=20, m=10 | 4.35m | 5.68m | –23 |
| D=10cm, d=1mm, n=50, m=4 | 3.88m | 4.16m | –6.7 |

Table 3: Analytical and numerical solutions for cylindrical coils.
Analytic solutions gives good estimates for coils longer than their diameter.

## A.2 Resistance and inductance of rectangular coil

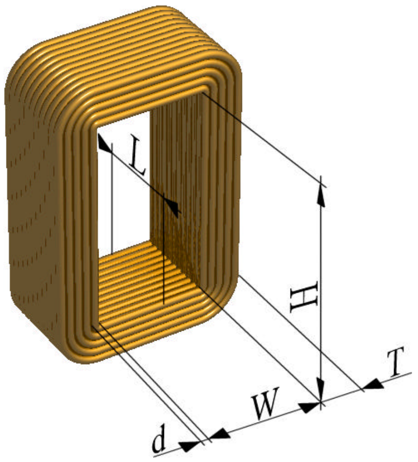


Figure 10: Geometry of a rectangular coil

| | |
|---|---|
| d | wire diameter |
| ϕ | diameter of wire's conductive area |
| $t_{isolation}$ | thickness of wire's isolation |
| l | total wire length |
| H | core height |
| L | core length |
| T | winding thickness |
| W | core width |
| m | # of layers |
| N | # of windings |
| n | # of windings per layer |

Table 4: Symbols

$$f = d - 2t_{isolation} \quad L = nd \quad T = md \quad N = mn$$

## Analytic calculation

The following formulas give a quick overview of coil characteristics. Analytically, the resistance R can be determined accurate again but the inductance L only at about ±20%.

Resistance: $R = r\,\dfrac{4l}{p f^2}$ where $l = N(pmd + 2H + 2W)$

$$R = r\,\frac{4N(pmd + 2H + 2W)}{p f^2} \tag{5}$$

Inductance:
$$L \approx m_0 \frac{HWN^2}{\sqrt{L^2 + HW}} \tag{6}$$

## Numeric calculation

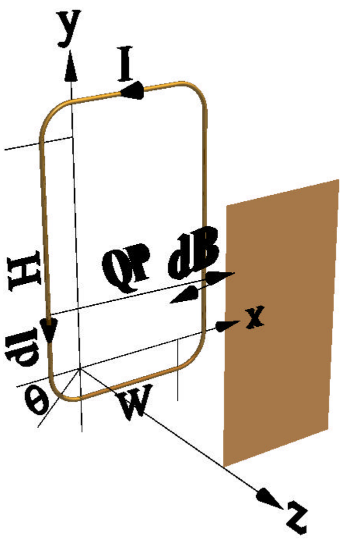


Figure 11: Contribution of current element d**l** at point Q to magnetic field d**B** at point P.

| | |
|---|---|
| I | current in wire |
| B | magnetic flux |
| R | winding radius in coins = distance from common section edges |
| x,y | planar position |
| θ | azimuth in coins |
| z | axial position |
| d**l** | current element |
| d**B** | magnetic flux incremental |
| **QP** | vector from current element to field point |

Table 5: Symbols

This time, the basic inductance equation [3] is applied to a rectangular inner section. The circumference of each winding can be divided into eight pieces – four linear pieces and four circular ones. Axial symmetry limits calculation to two linear pieces and one circular edge.

**Linear piece // x axis: Q:(0/-R/0)® (W/-R/0)**

Field point: $\overrightarrow{QP} = \begin{pmatrix} x - p \\ y + R \\ z \end{pmatrix}$

Wire element: $\vec{dl} = \begin{pmatrix} 1 \\ 0 \\ 0 \end{pmatrix} dp$

Axial flux: $\Phi_{x(R,z)} = \int\limits_{x=0}^{W} \int\limits_{y=0}^{H} \int\limits_{p=0}^{W} \dfrac{m_0 I}{4p} \dfrac{(y+R)dpdydx}{\left((x-p)^2 + (y+R)^2 + z^2\right)^{1.5}}$

**Linear piece // y axis: Q:(-R/H/0)® (-R/0/0)**

The development is nearly identical to that above.

Axial flux: $\Phi_{y(R,z)} = \int\limits_{x=0}^{W} \int\limits_{y=0}^{H} \int\limits_{p=0}^{H} \frac{m_0 I}{4p} \frac{(x+R)dpdydx}{\left((x+R)^2 + (y-p)^2 + z^2\right)^{1.5}}$

$\Phi_y$ can be deduced directly from $\Phi_x$ by commutation of variables and integration intervals. This will limit numerical implementation to one linear piece integration function.

**Circular piece:** **Q:(-R/0/0)® (0/-R/0)**

Field point: $\overrightarrow{QP} = \begin{pmatrix} x + R\cos q \\ y + R\sin q \\ z \end{pmatrix}$

Wire element: $\overrightarrow{dl} = \begin{pmatrix} \sin q \\ -\cos q \\ 0 \end{pmatrix} R dq$

Axial flux: $\Phi_{q(R,z)} = \int\limits_{x=0}^{W} \int\limits_{y=0}^{H} \int\limits_{q=0}^{p/2} \frac{m_0 I}{4p} \frac{(x\cos q + y\sin q + R)R dq dy dx}{\left((x + R\cos q)^2 + (y + R\sin q)^2 + z^2\right)^{1.5}}$

**Total axial flux:**

Summing up contributions of all m windings per axial section leads to:

$$\Phi_k = 2\sum_{i=0}^{m-1}\left(\Phi_{x((0.5+i)d,kd)} + \Phi_{y((0.5+i)d,kd)} + 2\Phi_{q((0.5+i)d,kd)}\right)$$

As in (4), finish by summing up over all axial sections:

$$\Phi_{tot} = m\sum_{i=0}^{n-1}\sum_{k=-i}^{n-1-i}\Phi_{|k|} = \underline{m\left(n\Phi_0 + 2\sum_{k=1}^{n-1}(n-k)\Phi_k\right)} \qquad (7)$$

It follows the listing of a *MatLab* function which approaches integrals by the piecewise trapezoidal integration formula:

```
% Determines inductance of a rectangular coil of inner
% width W, inner height H, wire diameter d, n windings
% per layer in each of the m layers.
%
function L=rectangularInductance(W, H, d, n, m)
if W < 0 | H < 0 | d < 0 | n < 1 | m < 1
   L=0;
else
   n=fix(n);
   m=fix(m);
   z=d*(0:n-1);
   R=d*(0.5+(0:m-1));
   L=2*(lineF(R, W, H, z)+lineF(R, H, W, z))+4*circF(R, W, H, z);
   if n == 1
      L=m/10^7*L;
   else
      L=m/10^7*L*[n 2*(n-1:-1:1)]';
   end;
end;

% Calculates flux contributions by circular edges of radius R
% in axial sections at positions z.
%
% Result vector gives flux for each axial section.
%
function f=circF(R, W, H, z)
z=z.^2;
dw=pi/20;
cw=cos(dw*(1:9));
sw=sin(dw*(1:9));
for k=1:length(z)
   n=8+fix(40/(1+z(k)/(H*W))^2);
   dB=zeros(n+1);
   dx=W/n;
```

```
   dy=H/n;
   x=dx*(0:n);
   y=dy*(0:n)';
   for l=1:length(R)
      cr=R(l)*cw;
      sr=R(l)*sw;
      a=x+R(l);
      b=y+R(l);
      dB=dB+repmat(a*R(l)/2,n+1,1)./real((repmat(a.^2,n+1,1)+
                                      repmat(y.^2+z(k),1,n+1))^1.5);
      dB=dB+repmat(b*R(l)/2,1,n+1)./real((repmat(x.^2,n+1,1)+
                                      repmat(b.^2+z(k),1,n+1))^1.5);
      for i=1:length(cr)
         a=repmat(x*cr(i),n+1,1)+repmat(y*sr(i)+R(l)^2,1,n+1);
         b=repmat((x+cr(i)).^2,n+1,1)+repmat((y+sr(i)).^2+z(k),1,n+1);
         dB=dB+a./b.^1.5;
      end;
   end;
   dB=(dB(1,:)+dB(n+1,:))/2+sum(dB(2:n,:));
   f(k)=dx*dy*dw*((dB(1)+dB(n+1))/2+sum(dB(2:n)));
end;

% Calculates flux contribution by linear sides for windings
% at distances R from inner section and for axial sections
% at positions z.
%
% Result vector gives flux for each axial section.
%
function f=lineF(R, W, H, z)
z=z.^2;
for k=1:length(z)
   n=8+fix(40/(1+z(k)/(H*W))^2);
   dx=W/n;
   dy=H/n;
   dB=zeros(n+1);
   for l=1:length(R)
      a=dx*(0:n)'+R(l);
      b=repmat(a,1,n+1);
      c=repmat(a.^2+z(k),1,n+1);
      dB=dB+(b./(c+repmat((dy*(0:n)).^2,n+1,1)).^1.5+
                                      b./(c+repmat((dy*(-n:0)).^2,n+1,1)).^1.5)/2;
      for i=1-n:-1
         dB=dB+b./(c+repmat((dy*(i:i+n)).^2,n+1,1)).^1.5;
      end;
   end;
   dB=(dB(1,:)+dB(n+1,:))/2+sum(dB(2:n,:));
   f(k)=dx*dy^2*((dB(1)+dB(n+1))/2+sum(dB(2:n)));
end;
```

## Comparison

| Coil layout | Analytic: L [H] | Numeric: L [H] | Relative error [%] |
|---|---|---|---|
| H=2cm, W=1cm, d=0.3mm, n=m=1 | 17.8n | 51.6n | –66 |
| H=2cm, W=1cm, d=0.3mm, n=10, m=1 | 1.74µ | 2.68µ | –35 |
| H=2cm, W=1cm, d=0.3mm, n=10, m=10 | 174µ | 193µ | –10 |
| H=2cm, W=1cm, d=0.3mm, n=14, m=9 | 271µ | 288µ | –5.9 |

Table 6: Analytical and numerical solutions for rectangular coils.
Again, analytic solution accuracy improves as coil length increases.

## A.3 Multiphase generator design

The subject of this section is to show the basic concepts for generator design. A bipolar generator poses little problems, but it is worth to spend some reflections for a multipolar/multiphase generator design. Here, multipolar refers to more than two magnetic poles and multiphase denotes several independent output voltages with arbitrary phase shift between them.

A multiphase system comprises necessarily multiple coils – no matter if connected or standalone [28]. Let n be the number of magnetic poles and m denote the number of coils in the system. Usually, one tends to arrange the poles and coils regularly on the circumference to have a geometric angle of 360°/n respective 360°/m between neighbours. It results a multiphase system with independent voltages and with an electrical phase shift of $\varphi = \pm 180° \cdot n/m$ between neighbours.

It sorts that a bipolar magnet system solely allows an arbitrary phase shift. Thus, why increase cost and use more magnetic poles?

Well, more magnetic poles means several magnetic and also electric periods a turn. One can multiply the phase frequency without change the rotation speed. Also, the coil's induction voltage increases and the system can benefit in form of saved space.

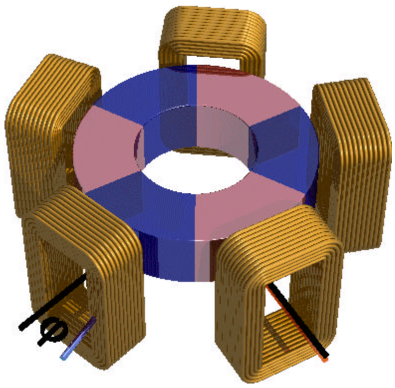


Figure 12: Multiphase generator

[28] If connected, connections form either a regular polygon or a star in almost every case – so spelled Δ or Y configuration.

# B. Mechanical design

## B.1 Centrifugal forces

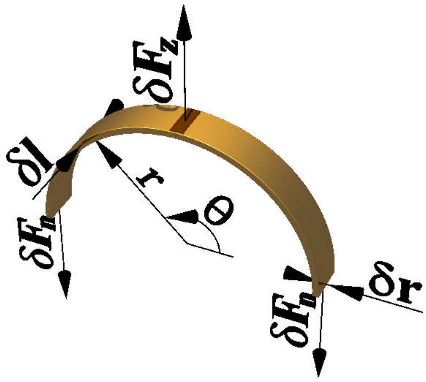


Figure 13: Strain on a cylindrical layer

| | |
|---|---|
| r | radius |
| θ | azimuth |
| δr | layer thickness |
| δl | layer length |
| $\delta F_n$ | normal force in section |
| $\delta F_z$ | centrifugal force |
| $a_z$ | centrifugal acceleration |
| $\sigma_n$ | azimuthal strain |
| ρ | mass density |
| ω | rotation speed |

Table 7: Symbols

### Analytic calculation

For a given rotation speed, the centrifugal acceleration $a_z$ on a mass at radius r from axis is:

$$a_z = \omega^2 r$$

The resulting force $\delta F_z$ on a layer element is then:

$$\delta F_z = \rho r a_z \delta l \delta r \delta \theta = \rho r^2 \omega^2 \delta l \delta r \delta \theta$$

Projection in direction of the normal forces $\delta F_n$ and integration leads to:

$$2\delta F_n = \int_{\theta=0}^{\pi} \sin(\theta) \delta F_z = 2\rho r^2 \omega^2 \delta l \delta r$$

The circular strain $\sigma_n$ in the layer section δlδr is finally calculated to:

$$\sigma_n = \frac{\delta F_n}{\delta l \delta r} = \underline{\rho r^2 \omega^2} \tag{8}$$

### Examples

| Layer of radius r [mm] at ω=2π·30krpm | $\sigma_n$ [MPa] for aluminium | $\sigma_n$ [MPa] for steel |
|---|---|---|
| 40 | 44 | 123 |
| 65 | 117 | 325 |
| 80 | 177 | 493 |

Table 8: Some sample values of azimuthal strain for aluminium alloys with $\rho_{Al}$≈2.8g/cm³ and iron alloys with $\rho_{Fe}$≈7.8g/cm³.

Note that formula **(8)** does not include radial strain. Therefore, effective azimuthal strain $\sigma_n$ will be reduced by the presence of radial strain $\sigma_z$.

## B.2 Part denominations and quantities

### B.2.1 Industrial available parts

| Number | Quantity | Denomination |
|---|---|---|
| 22 | 20 | Permanent NdFeB (Neodym) magnet parallelepiped 20mm x 10mm x 5mm<br>Magnetisation through thickness, geometric tolerance ±0.1mm to ±0.2mm<br>Maurer Magnetic AG<br>Industriestrasse 8<br>CH-8627 Arbon<br>http://www.maurermagnetic.ch/ |
| 23 | 4 | Permanent NdFeB (Neodym) magnet ring Ø40mm – Ø23mm x 6mm<br>Magnetisation in axis direction, geometric tolerance ±0.1mm to ±0.2mm<br>Magna-C GmbH<br>Bosslerstrasse 35<br>D-73240 Wendlingen<br>http://www.magna-c.de/ |
| 24 | 2 | High speed self lubricated glide bearing ISO 2795-10x16x10 sintered bronze 50<br>ITV Sintermetalle GmbH<br>Feldstrasse 5<br>Postfach 122<br>CH-8853 Lachen<br>http://www.itvsintermetalle.ch/ |
| 25 | 4 | Cylindrical bolt VSM 12´771-B4x16 |
| 26 | 4 | Ring spacer Ø4mm – Ø10mm x 4mm<br>A plastic ring fits well for easy length adjustment |
| 27 | 4 | Six pans screw without head ISO 4026-M3x6 |
| 28 | 2 | Six pans screw ISO 4762-M5x20 |
| 29 | 21 | Six pans screw ISO 4762-M5x25 |
| 30 | 24 | Disc DIN 125-B5 |
| 35 | 4 | Six pans screw without head ISO 4026-M3x10 |
| 36 | 5 | Six pans screw ISO 4762-M5x16 |

### B.2.2 Dedicated parts

| Number | Quantity | Denomination |
|---|---|---|
| 31 | 1 | Actuator coil N=24·10, d=0.34mm, D=41mm, L=8.1mm [29] |
| 32 | 1 | Supply coil N=12·22, d=0.34mm, L=4.2mm, H=20mm, W=10mm [30] |
| 33 | 2 | Sensor coil N=12·8, d=0.34mm, L=4.2mm, H=20mm, W=10mm |
| 34 | 8 | Power coil N=12·16, d=0.34mm, L=4.2mm, H=20mm, W=10mm |

The following pages outline all of the specially designed mechanical parts.

[29] Consult “A.1 Resistance and inductance of circular coil”.
[30] See “A.2 Resistance and inductance of rectangular coil”.

# C. Assemblage

All parts are referenced by their *names* and their {part numbers} [31].

This annexe suggests an assembly order recommended to follow.

## C.1 Motor

1. Put the *stator* on the *base* {13}.
2. Put the *lock* {12} over them.
3. Insert the *screws* {29} and tight them.
4. Stick the *rotor* onto the *axle* {15}.

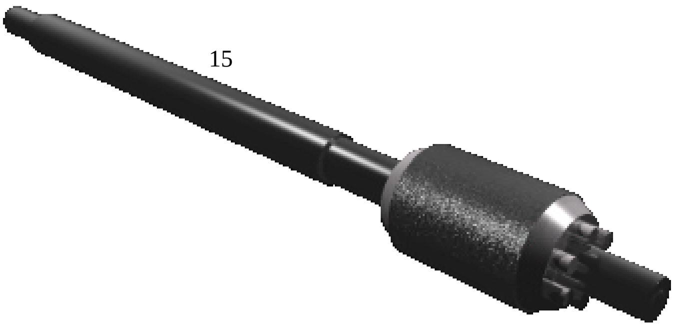


Figure 14: Axle

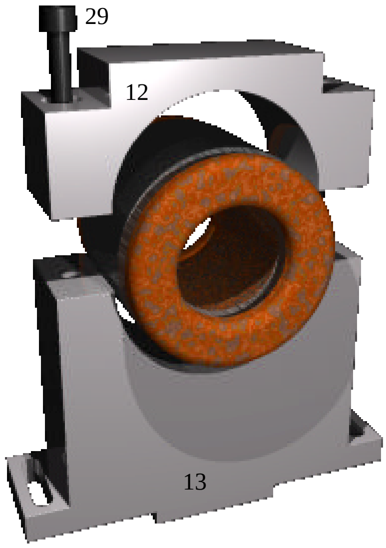


Figure 15: Motor base

## C.2 Base

1. Push the *glide bearings* {24} into their locations on the *axle supports* {16}.
2. Equip the *coil frame bases* {17} with adjustment *screws* {27 & 35}.
3. Place an *axle support* at the left side of the *base* {0} and fix it with *screws* {29/30}.
4. Place the *motor base* {13} next and fix it with *screws* {29/30}.
5. Put next a *coil frame base* with its opening to the right and fix it with *screws* {29/30}.
6. Insert the *axle* {15} into the *glide bearing*. Add the second *support* and adjust it to minimise the mechanical resistance between the *axle* and the *bearings*.
   Do manipulate the glide *bearings* with care. They must not be cleaned because they are filled with oil. Control the *axle*'s contact surfaces – if there is a little nut or spike, the *axle* will bite into the glide *bearing* and block.
7. Remove the *axle*.

[31] Consult the outlines of dedicated parts respective the trader references for industrial parts in "B.2 Part denominations and quantities".

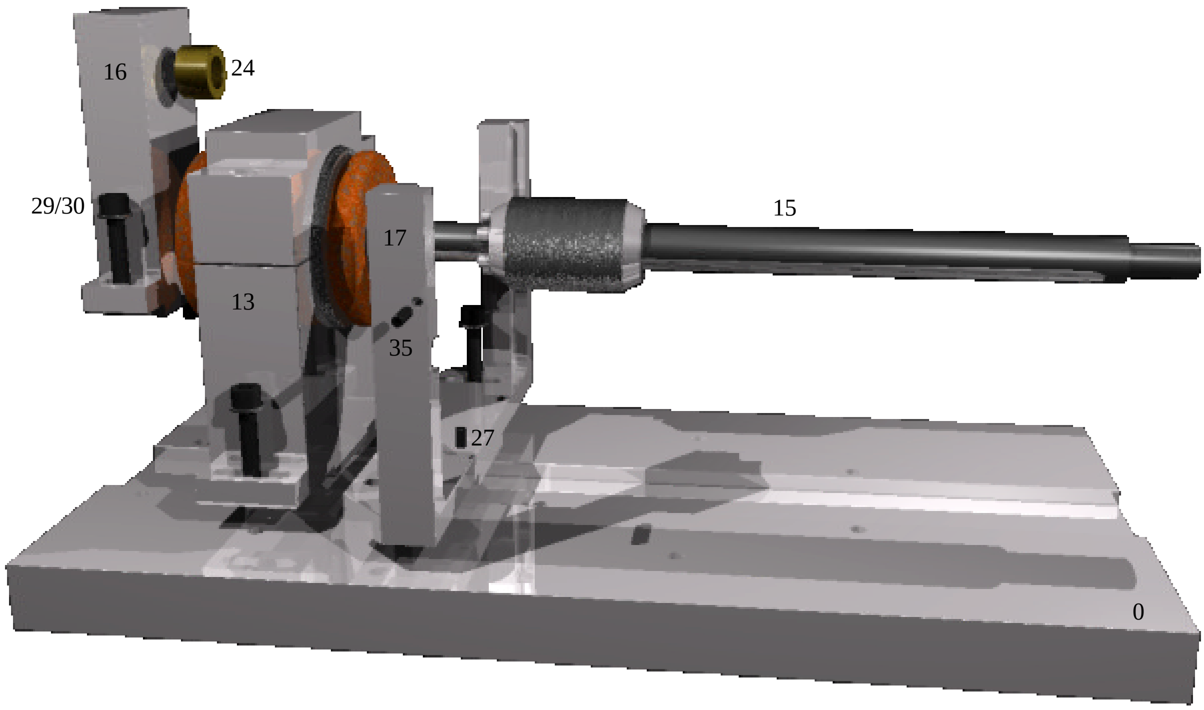


Figure 16: Base

## C.3 Generator

1. Prepare both *discs* {1 & 2}:
   Insert all *permanent magnets* {22} periodically with south respectively north pole up. To add the *shield* {3}, set it on one side of the *disc* and push it slowly to its final position. Caution: it will be pulled in its location! Once assembled, there is no way back.
2. Prepare both *coil frames* {14}:
   Stick the *supply coil* {32}, the *sensor coils* {33} and the *power coils* {34} into their locations. Exit all wires at the interior side of the *frames* – just the side where the extra spare was made to locate the *regulator supply coil* {32}. Prepare four *spacers* {26} by adjusting their heights – theoretically 2.2mm. Put the *frames* together by means of the *bolts* {25} and the *spacers*.
3. Push the *left disc* {1} onto the *axle* {15}.
4. Push the *bride cone* {9} onto the *axle* and pre-set its position.
   While shifting it over the *axle*, open it slightly with a screwdriver.
5. Place the *coil frames* {14}.
6. Push the *right disc* {2} onto the *axle*.
7. Insert the *screws* {29}:
   Tight them weakly because sole the magnetic attraction will be high enough to fix the generator.

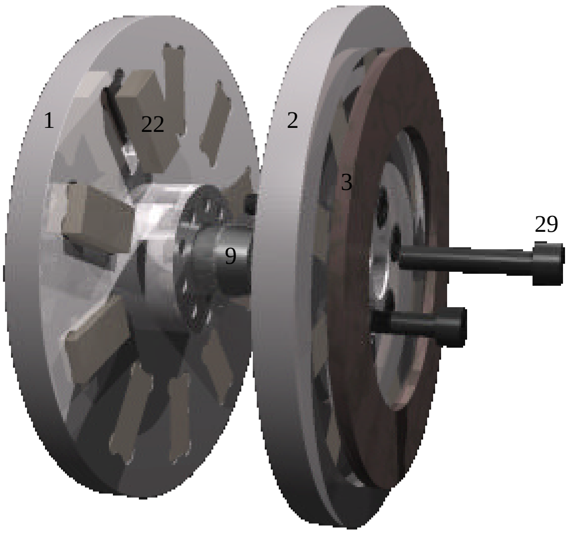


Figure 17: Generator discs

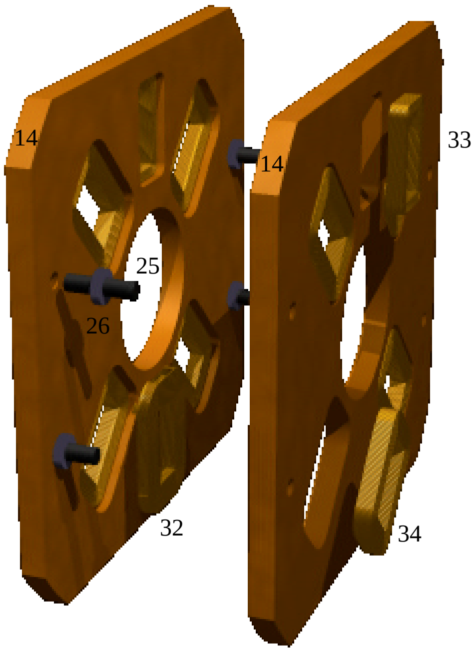


Figure 18: Generator coil frames

## C.4 Actuator

1. Stick the *actuator coil* {31} into its *frame* {11}.
   Exit the wires at the interior of a nut sawed into the inner T-shape.
2. Prepare the *magnet rings* {23}:
   Form two magnet pairs. Caution at your fingers! Place on each north pole one of the *inner pole shoes* {5}. Conversely, place on each south pole an *outer pole shoe* {6}. Align them coaxially by means of the *actuator base* {8} and the *spacer* {7}.
3. Push onto the *actuator base* the first *magnet pair* followed by the *spacer*. Add the *frame* and push the second *magnet pair* over them. Fix it with the *base cap* {4}.
4. Next, shift the parts onto the *axle* {15}.
5. Push the *bride cone* {9} onto the *axle* and preset its position.
   While shifting it over the *axle*, open it slightly with a screwdriver.
6. Add the *bride cap* {10} and fix it with *screws* {36}.

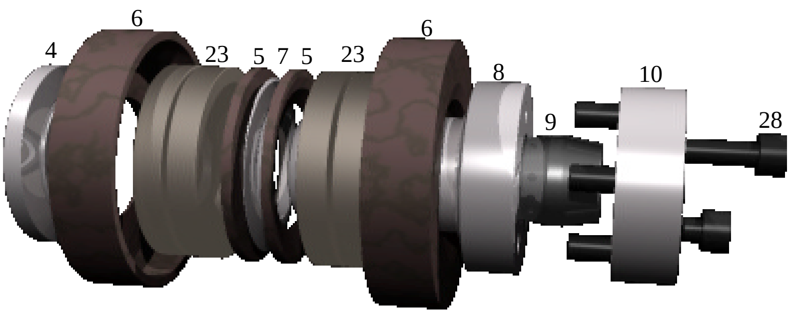


Figure 19: Actuator

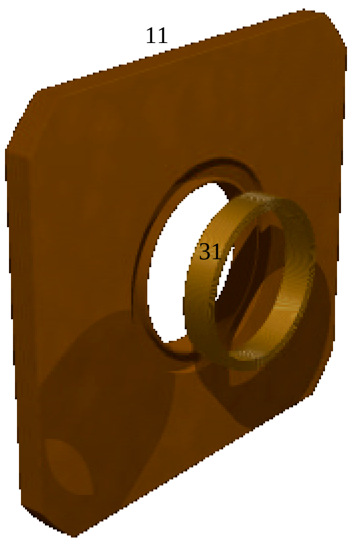


Figure 20: Actuator coil frame

## C.5 Finish

1. Insert the *axle* {15} into the *left bearing* {16}.
2. Add the right *axle support* {16} and fix it with *screws* {29/30} to give the axle a moving range of 2–3mm.
3. With the *screws* {27 & 35}, adjust the position of the *generator coil frames* {14}. Fix them with *screws* {29/30} in the *frame base* {17}.
4. Move the *frame base* to superpose the centres of the *generator discs* {1 & 2} and the *coil frames*.
5. Place the *actuator frame base* {17} with its opening to the left.
6. With the *screws* {27 & 35}, adjust the position of the *actuator coil frame* {11}. Fix it with *screws* {29/30} in the *frame base*.
7. Move the *frame base* to superpose the centres of the *actuator* and its *coil frame*.
8. Move the *motor base* {13} to superpose its *rotor* and *stator*.

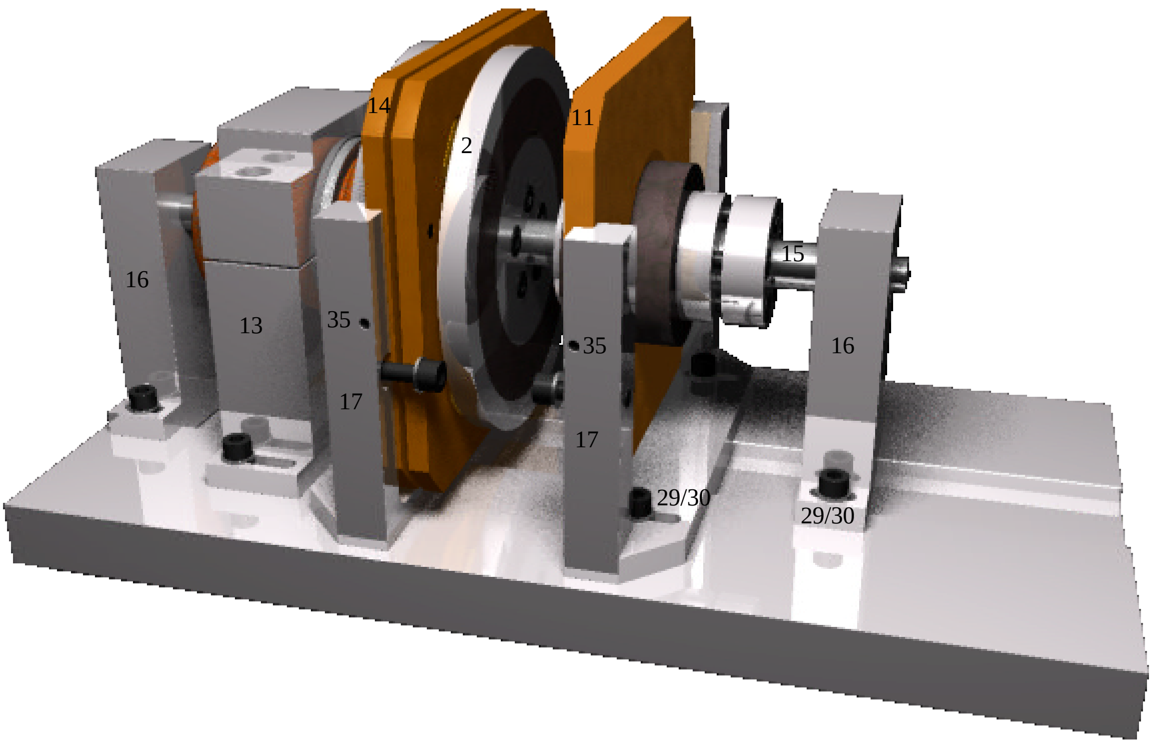


Figure 21: Complete demonstrator mechanics

## C.6 Mechanical tests

a) While moving the rotor over its axial range, it must not touch anything than the glide bearings.
b) The rotor has to turn without notable resistance.

# D. Circuit of signal processing unit

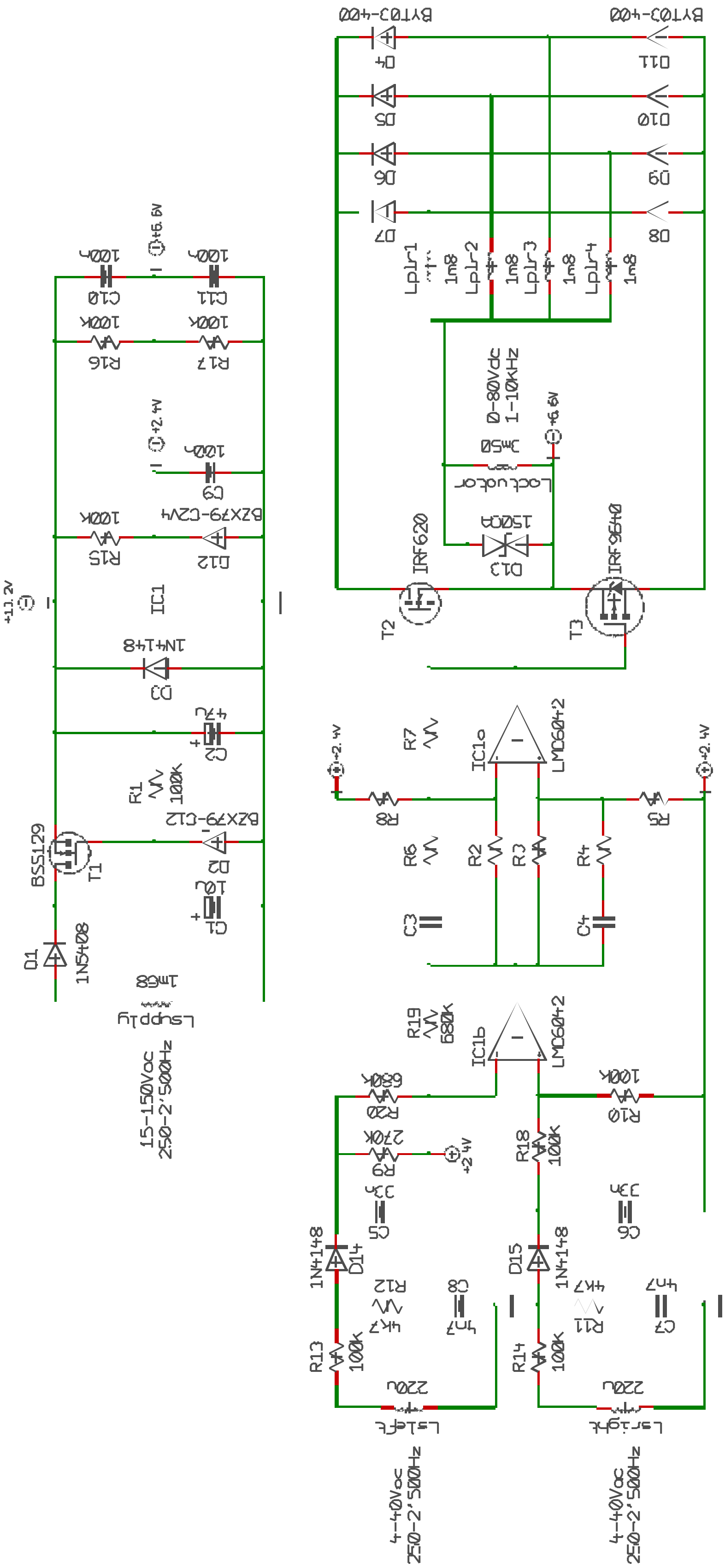


Schema 5: Entire circuit of signal processing unit [32].
Parts without values are interchangeable and are adapted by experimentation to obtain a reasonable behaviour of the position regulator. They are sensed for implementation of a proportional/differential regulator.

*BSS129* No datasheet available. Main characteristics: $U_{th}$=–1.5V, $U_{GS}$=±20V, $U_{DS}$=240V, $I_D$=50mA, $P_{tot}$=500mW.

32 Consult “G. Datasheets of semiconductor parts”.

# E. Measures

## E.1 Generator

| Geometry / Type | L=4.2mm, H=20mm, W=10mm / Windings N | Resistance R [Ω] Analytic | Resistance R [Ω] Measure | Inductance L [H] Analytic | Inductance L [H] Numeric | Inductance L [H] Measure |
|---|---|---|---|---|---|---|
| Position sensor | 93 | 1.53 | 1.7 ±0.2 | 147µ | 158µ | 220µ ±10µ |
| Actuator power | 192 | 3.56 | 3.7 ±0.2 | 628µ | 557µ | 945µ ±50µ |
| Circuit supply | 264 | 5.30 | 5.7 ±0.2 | 1.19m | 941µ | 1.68m ±85µ |

Table 9: Characteristics of rectangular coils with d=0.34mm wire [33].

The analytic calculation of the resistance is very accurate but for the inductance, neither the analytically nor the numerically calculated values match at less than 20% error. One can save the time spend for the numeric calculation, because the analytic solution seems to be of the same accuracy.

### Position sensor & circuit supply

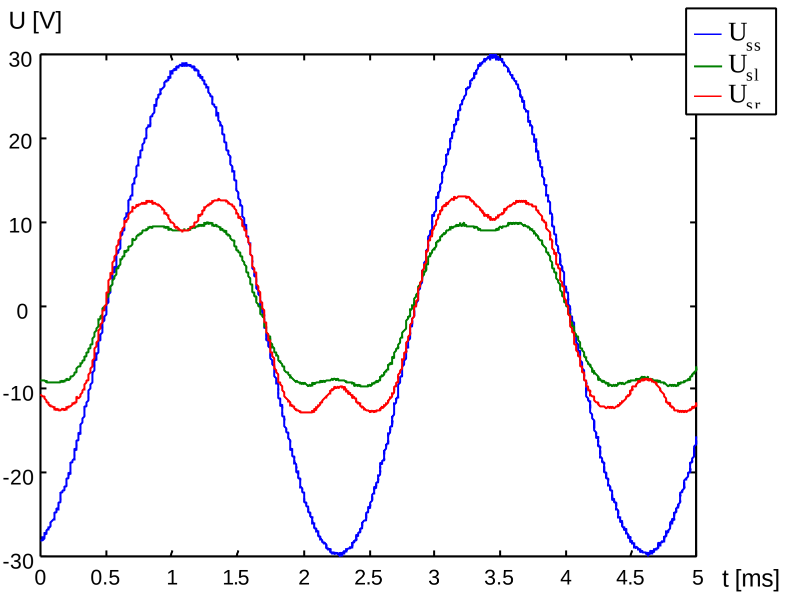


Graph 5: Voltages of the sensor coil pair @ 5´108rpm leftmost.
Also shown is the sinusoidal circuit supply voltage.

The right sensor coil has a significantly higher peak voltage than the left coil. This is needed for position recognition by the operation amplifier.

The supply coil furnishes a peak voltage of 5.8V/1´000rpm. After rectification, this voltage must be higher than 13V to enable the signal processing circuitry. The minimal rotation speed was designed to be 3´000rpm, thus giving about 17V. In fact, the circuitry goes operative at 2´400rpm.

The next graphs are just to show the transition of the sensor signals while the rotor moves to its rightmost position.

33 Refer to "A.2 Resistance and inductance of rectangular coil".

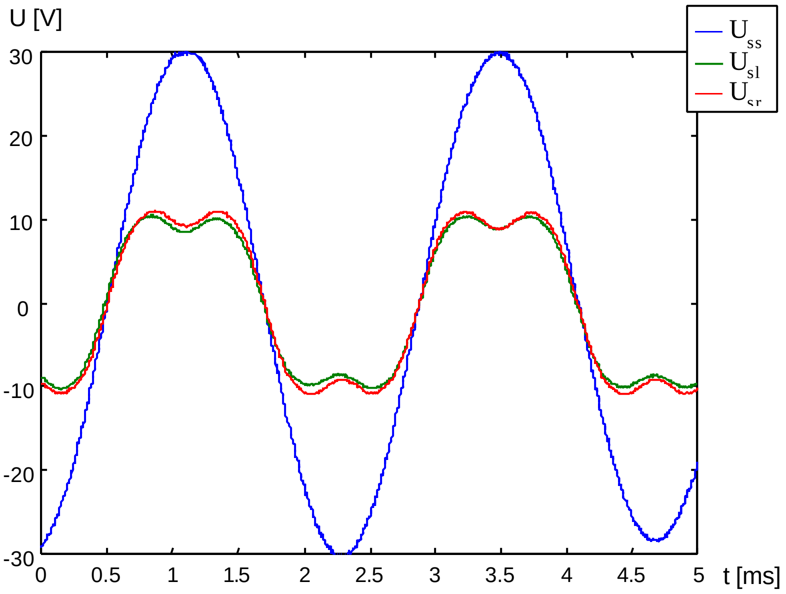


Graph 6: Voltages of the sensor coil pair @ 5´033rpm centred.

Note the invariance of the circuit supply voltage.

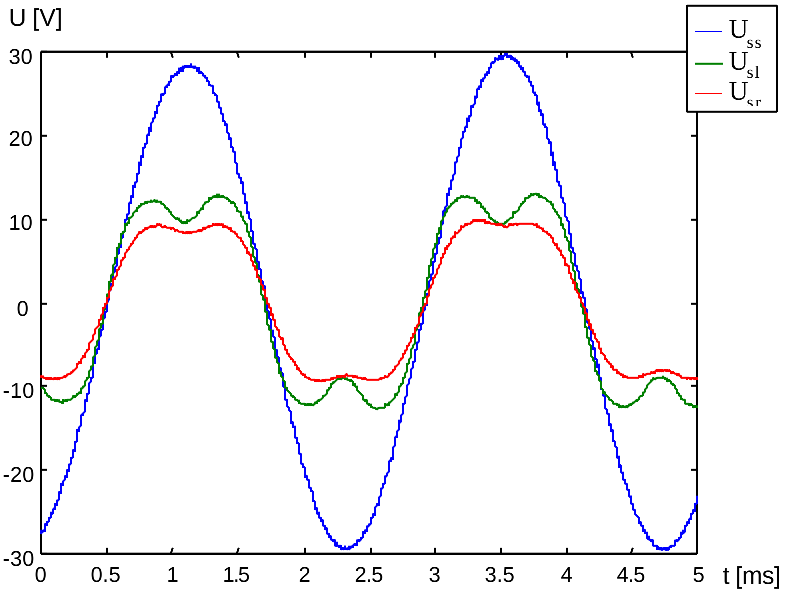


Graph 7: Voltages of the sensor coil pair @ 4´970rpm rightmost.

## Actuator power

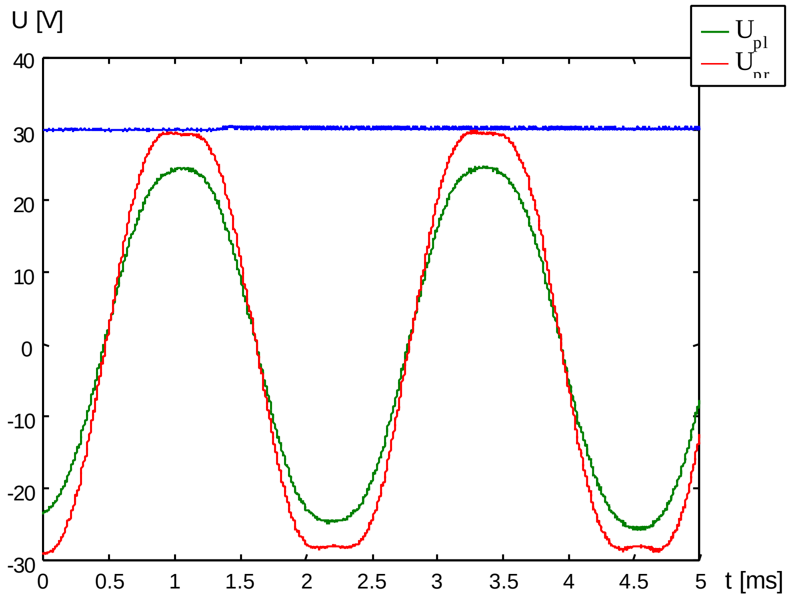


Graph 8: Voltages of a power coil pair [34] @ 5´178rpm leftmost.
Also shown is the rectified circuit supply voltage from which the voltage regulator draws <50µA to supply a constant voltage $U_{sc}$=13.2V±0.1V.

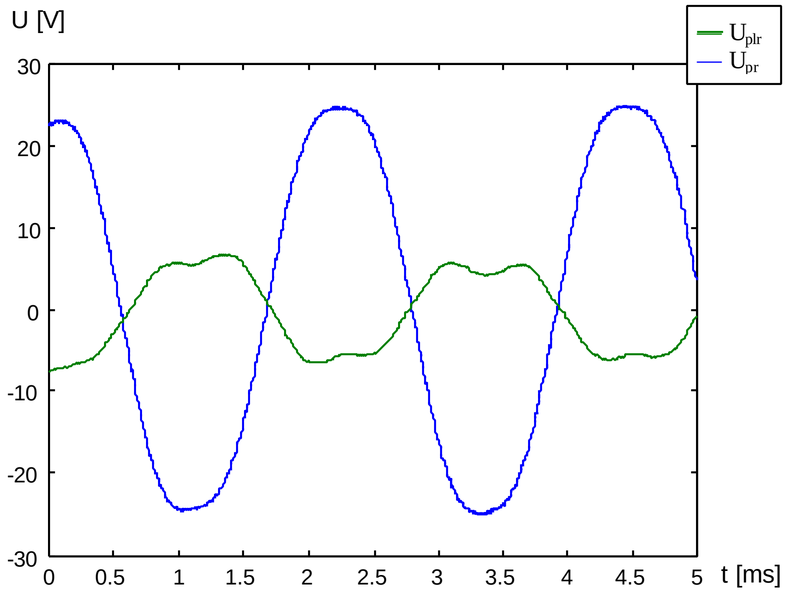


Graph 9: Differential versus single power coil voltage @ 5´418rpm leftmost.

[34] The power coil voltages were measured without load.

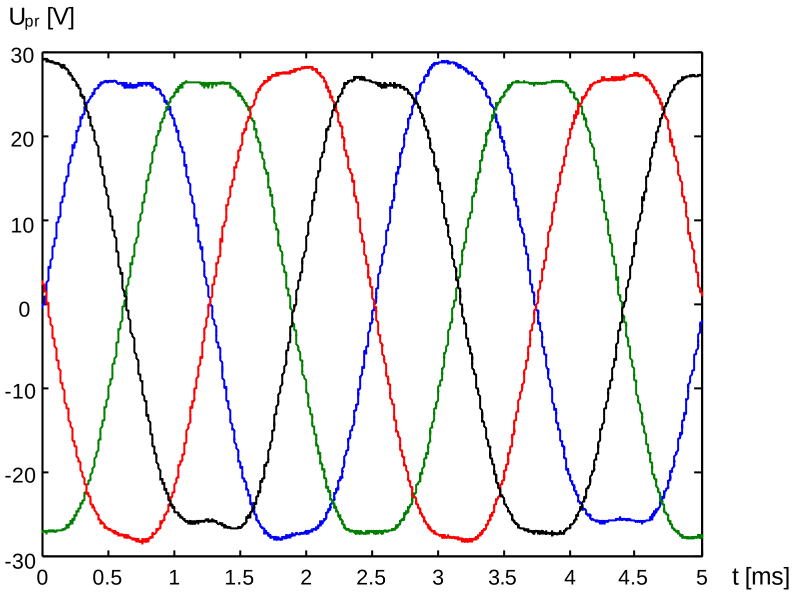


Graph 10: Voltages of right power coils @ 4´798rpm leftmost.
Note the phase shift of 90° between neighbours.

The power coils create a true RMS voltage of 4.0V/1´000rpm. The voltage shape is like predicted from the derivative of graph 3. After rectification and collection, the unified actuator voltage $U_{act}$=4.8V/1´000rpm has less than 20% ripple.

Besides, the above graph presents the effect of lazy alignment of the generator coils and permanent magnets. The overshot of the thicker black and blue lines indicate a single magnet nearer to the coils. On the other hand, the red line indicates a coil placed somewhat closer to the magnets. It was known in prior that these errors do not degrade the function significantly.

### Conclusions

The generator does behave like predicted. Its outputs match the required voltages, shape and phase.

The input stages of the signal processing circuit passed the initial function test – the linear voltage regulator and the sensor signal conditioning stages are ok. The operation amplifier and the output stage were revised and found ok before they were connected to the actuator and its power supply coils.

## E.2 Actuator

| Geometry / Type | L=8.1mm, D=41mm / Windings N | Resistance R [Ω] Analytic | Resistance R [Ω] Measure | Inductance L [H] Analytic | Inductance L [H] Numeric | Inductance L [H] Measure |
|---|---|---|---|---|---|---|
| Actuator | 235 | 7.88 | 8.2 ±0.2 | 2.64m | 3.28m | 3.50m ±180µ |

Table 10: Characteristics of circular coil with d=0.34mm wire [35].

Again, the resistance is calculated accurate. This time, the numerical integration of the inductance was useful, because the committed error diminishes significantly compared to the analytic formula.

After the assembly of the actuator, the inductance was found to be the same. This indicates that the ferromagnetic material is well saturated and therefore offers no permeability gain.

[35] Details in "A.1 Resistance and inductance of circular coil".

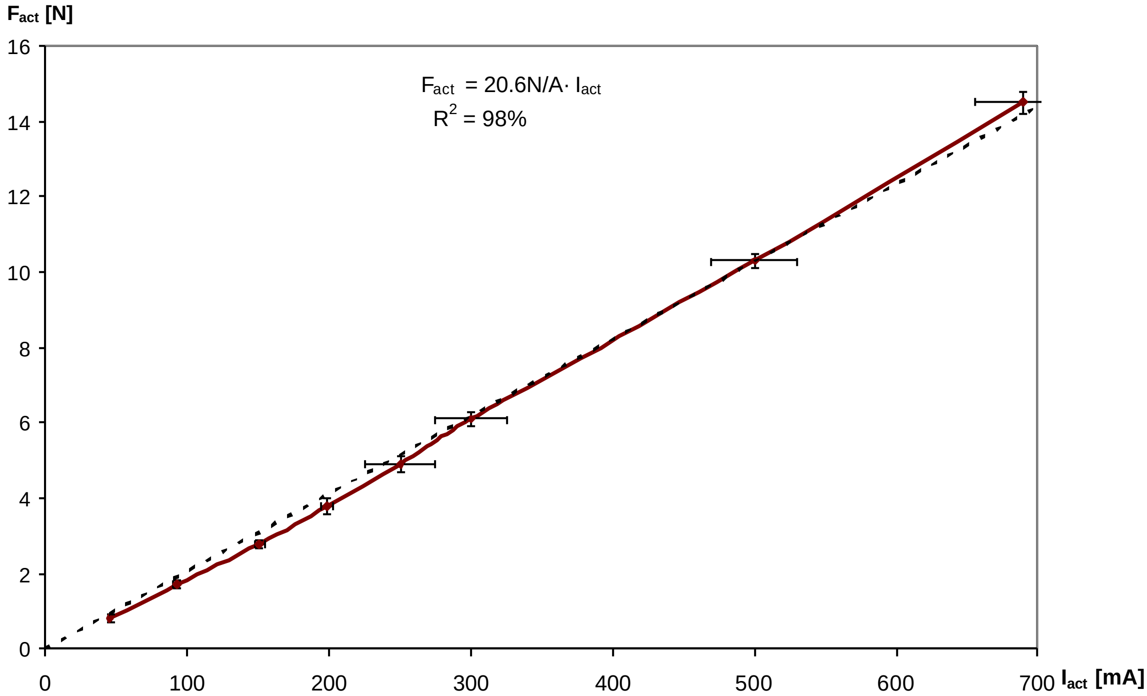


Graph 11: Actuator force–current ratio.
The rotor turned at the centred position. The current was imposed by a DC voltage source and measured by a standard multimeter. The force was imposed through a lever – one end pushed onto the axle while the other was pulled with a Newton meter. To measure the force, the motor was switched off and the rotor maintained at its centred position. Note that the generator did not supply any power.

Note the fairly well linear proportionality. As formerly mentioned, the actuator force is nearly position independent. In fact, a slight decrease of 2% to 5% for ±1mm rotor excursion was observed.